ORIGINAL ARTICLE

Na+-D-glucose Cotransporter SGLT1 is Pivotal for Intestinal Glucose Absorption and Glucose-Dependent Incretin Secretion

Valentin Gorboulev,[1] Annette Schürmann,[2] Volker Vallon,[3] Helmut Kipp,[1] Alexander Jaschke,[2] Dirk Klessen,[1] Alexandra Friedrich,[1] Stephan Scherneck,[2] Timo Rieg,[3] Robyn Cunard,[3] Maike Veyhl-Wichmann,[1] Aruna Srinivasan,[1] Daniela Balen,[4] Davorka Breljak,[4] Rexhep Rexhepaj,[5] Helen E. Parker,[6] Fiona M. Gribble,[6] Frank Reimann,[6] Florian Lang,[5] Stefan Wiese,[7] Ivan Sabolic,[4] Michael Sendtner,[8] and Hermann Koepsell[1]

To clarify the physiological role of Na+-D-glucose cotransporter SGLT1 in small intestine and kidney, $Sglt1^{-/-}$ mice were generated and characterized phenotypically. After gavage of D-glucose, small intestinal glucose absorption across the brush-border membrane (BBM) via SGLT1 and GLUT2 were analyzed. Glucose-induced secretion of insulinotropic hormone (GIP) and glucagon-like peptide 1 (GLP-1) in wild-type and $Sglt1^{-/-}$ mice were compared. The impact of SGLT1 on renal glucose handling was investigated by micropuncture studies. It was observed that $Sglt1^{-/-}$ mice developed a glucose-galactose malabsorption syndrome but thrive normally when fed a glucose-galactose–free diet. In wild-type mice, passage of D-glucose across the intestinal BBM was predominantly mediated by SGLT1, independent the glucose load. High glucose concentrations increased the amounts of SGLT1 and GLUT2 in the BBM, and SGLT1 was required for upregulation of GLUT2. SGLT1 was located in luminal membranes of cells immunopositive for GIP and GLP-1, and $Sglt1^{-/-}$ mice exhibited reduced glucose-triggered GIP and GLP-1 levels. In the kidney, SGLT1 reabsorbed ~3% of the filtered glucose under normoglycemic conditions. The data indicate that SGLT1 is *1*) pivotal for intestinal mass absorption of D-glucose, *2*) triggers the glucose-induced secretion of GIP and GLP-1, and *3*) triggers the upregulation of GLUT2. *Diabetes* **61:187–196, 2012**

O besity, type 2 diabetes, and the metabolic syndrome are some of the major medical and economical challenges of modern societies. Dysregulation of carbohydrate management, increased consumption of carbohydrates and fat, and reduced insulin receptor sensitivity contribute to the metabolic derangements. Drugs that reduce small intestinal uptake of D-glucose and/or reabsorption of D-glucose from the renal filtrate or that modulate secretion of insulinotropic enterohormones can provide new therapeutic strategies (1,2). To further explore these options a better understanding of the underlying molecular mechanisms is required.

The primary transporters that mediate transcellular movements of D-glucose in small intestine have been identified and include the Na+-D-glucose cotransporter SGLT1 and GLUT2 (3,4). It is generally accepted that SGLT1 mediates uptake of low concentrations of D-glucose across the brush-border membrane (BBM) of the small intestine and that D-glucose leaves enterocytes across the basolateral membrane (BLM) via GLUT2 (3). However, their relative contributions to D-glucose absorption after a carbohydrate-rich meal remain controversial (5–7). Kellet and coworkers suggested that under these conditions GLUT2 is incorporated into the BBM allowing mass absorption of D-glucose via GLUT2 (5,6,8). However, the observation that small intestinal mass absorption of D-glucose in mice was not significantly changed when GLUT2 was removed (9) contradicts this hypothesis.

Among other dietary stimulants, D-glucose can trigger the intestinal secretion of glucose-dependent insulinotropic peptide (GIP) by K-cells as well as the secretion of glucagon-like peptide 1 (GLP-1) by L-cells (10–12). Potential glucose sensing systems expressed in these enteroendocrine cells include sweet taste receptors and glucose transporters like SGLT1, but their roles in glucose-induced secretion of GLP-1 and GIP have not been fully established (7,13–16).

There is agreement that the bulk of D-glucose filtered in the glomeruli of the kidney is reabsorbed in the S1 and S2 segments of proximal tubules via SGLT2 in the BBM and GLUT2 in the BLM (17), and it is generally assumed that the remaining glucose is reabsorbed in the S2 and S3 segments via SGLT1 in BBM and GLUT1 in the BLM. However, the physiological significance and quantitative contribution of SGLT1 for renal reabsorption of D-glucose has not been directly determined (17).

In the present work we generated and characterized the phenotype of an $Sglt1^{-/-}$ mouse model to gain new insights. We report that these mice show symptoms of the glucose-galactose malabsorption (GGM) syndrome (OMIM 182380) that appears to be cured by a diet low in glucose and galactose (18,19). The experiments identify SGLT1 as the primary pathway for the transport of D-glucose across the BBM during D-glucose mass absorption and show that

SGLT1 is essential for the glucose-induced release of GIP and GLP-1 into the peripheral circulation. Finally, we establish a small but significant contribution of SGLT1 to renal D-glucose reabsorption under normoglycemic conditions.

RESEARCH DESIGN AND METHODS

Animal handling. Mice were handled in compliance with Institutional guidelines and German, U.K., and U.S. laws. Comparison between $Sglt1^{-/-}$ and wild-type mice was performed between the 8th and 12th generation of backcrossing of $Sglt1^{-/-}$ (129/OLA/C57BL/6 background) with wild-type (C57BL/6 background). Animals were kept in a temperature-controlled environment with a 12-h–light/12-h–dark cycle.

Diets. Standard maintenance chow (Ssniff V1534–000 R/M-H, 10 mm) was obtained from Spezialdiäten GmbH, Soest, Germany. It contained 12.8 MJ kg^{-1} metabolizable energy and was composed of 36.4% starch, 19% protein, 4.9% fiber, 4.7% mono- and disaccharides, and 3.3% fat, minerals, and vitamins. The glucose-galactose–free diet was prepared by Altromin Spezialfutter GmbH (Lage, Germany) and contained 13.2 MJ kg^{-1} metabolizable energy. It was composed of 33.8% protein, 30.7% fiber, and 20.5% fat, minerals, and vitamins.

Antibodies. The antibodies used are described in Table 1.

Immunohistochemistry. Immunofluorescence histochemistry was performed with cryo-sections of p-formaldehyde–fixed tissue as described (22). For double staining sections were first incubated with GIP-Ab or GLP-1-Ab and respective secondary antibody and washed. Thereafter sections were incubated overnight at 4°C with SGLT1-Ab, rinsed with PBS, incubated with GAR-AF555 for 60 min at room temperature, and washed. Laser scanning fluorescence microscopy was performed with a confocal laser-scanning imaging system, LSM-510 using the argon laser for green fluorochromes (λ_{ex} = 488 nm, LP505 nm), and the helium-neon laser for red fluorochromes (λ_{ex} = 543 nm, BP560–615 nm) (Zeiss, Jena, Germany). The Zeiss LSM-510 software 2.5 SP2 stack, multi track, 8 bit scan mode was used.

Gavage with glucose and oil. After a 16- to 18-h fasting period mice were gavaged with a 10% D-glucose solution (2 mg/g body wt) in PBS, a 40% D-glucose solution (6 mg/g body wt) in PBS, or with olive oil (10 μL/g body wt). Control animals were gavaged with PBS.

Measurements of glucose, insulin, and enterohormones in the plasma. For determination of D-glucose and insulin blood was collected from the tail. Concentrations of D-glucose were determined with an Ascensia CONTOUR Meter using Ascensia MICROFIL Test Strips (Bayer Vial GmbH, Leverkusen). Insulin levels were measured with the Insulin (Mouse) Ultrasensitive EIA from ALPCO Diagnostics (Salem, NH). For determination of enterohormones, mice were anesthetized with isoflurane and blood was collected after heart tap. For GLP-1 determination blood was immediately mixed with a dipeptidyl peptidase (DPP)-IV inhibitor yielding a final concentration of 100 μmol/L (Millipore Corporation, Billerica, MA). Active GLP-1 was determined by an ELISA kit supplied by Millipore Corporation (GLP-1(7–36) active, kit EGLP-35 K) (Fig. 5C). Total GLP-1 was determined by an ELISA kit provided by MesoScale

Discovery (Gaithersburg, MD; kit K150JVC-4; Fig. 5D and Supplementary Fig. 5B). GIP was determined by an ELISA kit obtained from Millipore Corporation that is specific for both active GIP (1–42) and inactivated GIP (3–42) of rat and mouse (kit EZRMGIP-55 K).

Preparation of BBM vesicles from small intestine. Mice were killed 30 min after gavage. BBM vesicles (BBMVs) were isolated by magnesium precipitation followed by differential centrifugation. Small intestines of three mice were homogenized in 35 mL of homogenization buffer (100 mmol/L mannitol, 2 mmol/L HEPES/Tris [pH 7.1]). MgCl$_2$ solution (1 mol/L) was added to a concentration of 10 mmol/L, and the suspension was kept on ice for 20 min. After 15 min centrifugation at 3,000 g, the pellet containing nuclei and mitochondria was discarded. The supernatant was centrifuged for 30 min at 27,000 g, and the resulting pellet was suspended in 35 mL vesicle buffer (100 mmol/L mannitol, 20 mmol/L HEPES/Tris [pH 7.4]). After 30 min centrifugation at 27,000 g, the pellet was suspended in 300 μL vesicle buffer. The BBMVs were snap-frozen in liquid nitrogen and stored at −70°C until use.

Glucose uptake into BBMVs. BBMVs were thawed in a water bath, and uptake of radiolabeled substrates was determined at 22°C using the rapid filtration technique (23). To measure sodium-dependent and phlorizin-inhibitable uptake of α-methyl-D-glucoside (AMG), vesicles were incubated with vesicle buffer containing 0.1 mmol/L [^{14}C]AMG plus either 100 mmol/L NaSCN or 100 mmol/L NaSCN plus 0.2 mmol/L phlorizin or 100 mmol/L KSCN. Uptake was stopped with ice-cold vesicle buffer containing 100 mmol/L NaSCN plus 0.2 mmol/L phlorizin (stop solution), and vesicles were washed on nitrocellulose filters with stop solution. The radioactivity on the filters was measured and phlorizin-inhibitable or sodium-dependent AMG uptake was calculated. To measure GLUT2-mediated D-glucose uptake, which is inhibited by glucosamine (24), BBMVs were incubated for 1 min at 22°C with 20 mmol/L HEPES/Tris [pH 7.4] containing 100 mmol/L [^{3}H]-D-glucose plus 100 mmol/L mannitol or plus 100 mmol/L D-glucosamine. Uptake was stopped with ice-cold 20 mmol/L HEPES/Tris [pH 7.4] containing 100 mmol/L mannitol plus 100 mmol/L D-glucosamine, and vesicles were washed on nitrocellulose filters.

Glucose uptake into everted rings. Everted rings of duodenum and jejunum were incubated for 2 min in Krebs-Ringer buffer containing 7 μmol/L [^{14}C]AMG without and with 0.2 mmol/L phlorizin. Uptake was stopped with ice-cold Ringer buffer containing 0.2 mmol/L phlorizin. The length of individual segments was measured under a microscope, the segments were solubilized, and radioactivity was analyzed.

Glucose uptake by SGLT1 expressed in oocytes. SGLT1 was expressed in oocytes of Xenopus laevis, and measurements of AMG uptake were performed as described (25). The cDNA of mouse Sglt1 (accession number BC003845) was cloned into the vector pRSSP, and m7G(5′)G-capped cRNA was prepared. Oocytes were injected with 5 ng of mouse Sglt1 cRNA and incubated 2 days for expression. For transport measurements the oocytes were incubated for 20 min at room temperature with [^{14}C]AMG or [^{3}H]D-glucose in the absence and presence of 100 μmol/L phlorizin, and phlorizin-inhibited uptake was analyzed.

Renal glucose reabsorption. Glomerular filtration rate (GFR) and renal glucose reabsorption were determined in awake and anesthetized mice as described previously (20,26,27).

TABLE 1
Description of antibodies

Name	Antigen	Host	Source (Cat. No.)	Properties (use)
SGLT1-Ab[1]	mouse SGLT1, aa 586 to 601 (KDTIEIDTEAPQKKKKG)	Rabbit	raised for this study	see article (pA, WB, IH)
SGLT2-Ab[1]	rat SGLT1, aa 592–609 (AMGIEEVQSPAPGLLRQC)	Rabbit	raised previously (20)	cross-reacts with mouse SGLT2 (pA, WB, IH)
GLUT2-Ab	peptide of human GLUT2 (pep C-19, from COOH terminus)	Goat	Santa Cruz Biotechnology (sc-7580)	cross-reacts with mouse GLUT2 (21) (pA, WB, IH)
GIP-Ab	human GIP (pep Y-20, from internal region)	Goat	Santa Cruz Biotechnology (sc-23554)	cross-reacts with mouse GIP (pA for IH)
GLP-1-Ab	human GLP-1 (pep C-17, from COOH terminus)	Goat	Santa Cruz Biotechnology (sc-7782)	cross-reacts with mouse GLP-1 (pA, IH)
GAR-AF555	rabbit IgG	Goat	Invitrogen GmbH (A21428)	Alexa Fluor 555-labeled (sA, IH)
CAG-488F	goat IgG	Chicken	Invitrogen GmbH (A21467)	Alexa Fluor 488-labeled (sA, IH)
DAR-HRP	rabbit IgG	Donkey	Dianova (711–035–152)	Horseradish peroxidase-labeled (sA, WB)
DAG-HRP	goat IgG	Donkey	Dianova (705–035–147)	Horseradish peroxidase-labeled (sA for WB)

aa, Amino acids; WB, Western blot; IH, immunohistochemistry; pA, primary antibody; pep, peptide; sA, secondary antibody. [1]Affinity-purified via the respective antigenic peptide as described (20).

RESULTS

Removal of SGLT1 leads to GGM syndrome. The strategy to generate mice lacking part of the *Sglt1* promotor and the first exon of *Sglt1* is outlined in Supplementary Fig. 1*A*. *Sglt1*$^{+/-}$ mice and *Sglt1*$^{-/-}$ mice were identified by Southern blots and PCR (Supplementary Fig. 1*B* and *C*). To verify effects on glucose transport, we expressed murine *Sglt1* or murine *Sglt1* mutant without exon 1 in *Xenopus laevis* oocytes and measured phlorizin (100 µmol/L)-inhibitable uptake of 50 µmol/L AMG, a SGLT-specific substrate that is not transported by GLUT transporters. Whereas a high transport activity was observed after expression of SGLT1 wild type, no significant AMG uptake was observed with the SGLT1 mutant (Supplementary Fig. 2). Breeding of *Sglt1* heterozygote mice demonstrated Mendelian type inheritance (from 531 outcomes 51% were heterozygotes, 27% wild type, and 22% *Sglt1*$^{-/-}$), indicating embryonic survival of *Sglt1*$^{-/-}$ mice. Whereas preweaning *Sglt1*$^{-/-}$ mice appeared to be healthy, *Sglt1*$^{-/-}$ mice died within 2 days after weaning when they received standard diet. In contrast, weaned *Sglt1*$^{-/-}$ mice survived well and were fertile when they were fed a diet that did not contain free monosaccharides and disaccharides (Fig. 1*A*). To determine whether the inactivation of *Sglt1* in mice induced a GGM syndrome as in humans (19), two-month-old mice fed with glucose-galactose–free diet were transitioned to standard diet (Fig. 1*B*). Whereas wild-type mice did not show a significant change in weight, the *Sglt1*$^{-/-}$ mice appeared unwell after 2 days, became weaker, lost body weight, and died within 7 to 12 days after the dietary change (Fig. 1*B*). Laparatomy 2 days after reapplication of standard diet revealed distended small and large intestines in the *Sglt1*$^{-/-}$ mice (Fig. 1*C*). Absence of *Sglt1* mRNA and SGLT1 protein in the small intestine of *Sglt1*$^{-/-}$ mice was verified by Northern blotting, Western blotting, and immunohistochemistry (Fig. 1*D–F*).

To determine the contribution of SGLT1 to Na$^+$-D-glucose cotransport across BBM of small intestine we compared AMG uptake across the BBM of wild-type versus *Sglt1*$^{-/-}$ mice. Comparison was performed in mice fed a glucose-galactose–free diet. Three methods were used: measurement of phlorizin-inhibitable AMG uptake into everted rings of small intestine (Fig. 1*G*), measurement of glucose-induced short circuit currents across small intestinal mucosa (Fig. 1*H*), and measurement of phlorizin-inhibitable AMG uptake into isolated BBMVs (Fig. 2*C*). The data show that absence of SGLT1 abolishes Na$^+$-D-glucose cotransport across the small intestinal BBM. Mice express SGLT1 homologs SGLT3a and SGLT3b (30). Confirming recently reported data (30), we observed phlorizin-inhibitable uptake of AMG after expression of SGLT3b in oocytes of *Xenopus laevis*. By comparison, phlorizin-inhibitable AMG uptake could not be detected after expression of SGLT3a (Supplementary Fig. 3*A*). Using immunohistochemistry we observed immunoreactivity of an antibody raised against SGLT3b at the BBM of small intestinal enterocytes (Supplementary Fig. 3*B*). The functional data in BBMs, however, indicate that SGLT3b activity cannot substitute for SGLT1.

Small intestinal mass absorption of D-glucose across the BBM is mainly mediated by SGLT1. Kellet and coworkers raised the hypothesis that at high luminal glucose concentrations GLUT2 is incorporated into the BBM and is the dominant pathway for D-glucose translocation across the BBM under these conditions (5,6,8). These

authors postulated that the incorporation of GLUT2 into the BBM is triggered by SGLT1 activity leading to activation of the Ca^{2+} channel Ca$_v$1.3 (5,8). However, in a more recent review it was proposed that Ca$_v$1.3 is activated by sweet taste receptors and endocrine and paracrine hormones including insulin (6).

We compared the increase of plasma D-glucose concentrations after gavage of a solution containing D-glucose (2 mg/g body wt) in wild-type versus *Sglt1*$^{-/-}$ mice (Fig. 2*A*). In wild-type mice the increase of D-glucose concentrations in plasma was significantly higher than in *Sglt1*$^{-/-}$ mice (3.3-fold vs. 1.8-fold after 13 min). The increase of plasma D-glucose after glucose gavage in *Sglt1*$^{-/-}$ mice (1.8 ± 0.2-fold) was similar in magnitude to the increase observed in *Sglt1*$^{-/-}$ mice (1.8 ± 0.1-fold) and wild-type mice (1.7 ± 0.1-fold) after gavage of solvent control (Fig. 2*A*) and may reflect stress (adrenalin)-induced release of D-glucose from the liver. These data provide evidence that SGLT1 is required for small intestinal mass absorption of D-glucose.

To determine whether D-glucose transport across the BBM after a glucose bolus is mediated by SGLT1 or GLUT2 we performed studies with BBMVs from wild-type and *Sglt1*$^{-/-}$ mice. About 10-fold higher K_m values were obtained for SGLT1-mediated uptake of D-glucose/AMG across small intestinal BBMs of wild-type mice compared with values obtained from *Xenopus* oocytes expressing mouse SGLT1 (Fig. 3). BBMVs were prepared from mice gavaged with PBS or PBS containing D-glucose (6 mg/g body wt) and killed 30 min later. Whereas in BBMVs of wild-type mice, which received the glucose bolus, the K_m value of sodium-dependent AMG uptake was modestly (25%) reduced compared with wild-type mice receiving only PBS (Fig. 2*B*), the V_{max} value of AMG uptake was 4.4-fold increased (Fig. 2*C*). The corresponding amount of SGLT1 protein in BBMVs estimated from Western blots was increased 2.4-fold (Fig. 2*D*). In BBMVs of *Sglt1*$^{-/-}$ mice no uptake of the SGLT specific substrate AMG was detectable without and with D-glucose gavage (Fig. 2*C*). The data indicate upregulation of SGLT1 expression in the BBM after gavage with D-glucose in mice.

Maximal transport activity (V_{max}) of GLUT2 across the BBM was determined by measuring the uptake of 100 mmol/L D-glucose (partially [^{3}H]-labeled) that could be blocked by the GLUT2 specific inhibitor glucosamine (100 mmol/L) (24). In oocytes expressing mouse SGLT1 we verified that glucosamine does not inhibit SGLT1 (Supplementary Fig. 4). V_{max} of GLUT2-mediated D-glucose uptake into BBMVs in wild-type mice without glucose gavage was similar to *Sglt1*$^{-/-}$ mice without or with glucose gavage (43–70 pmol × mg^{-1} × s^{-1}; Fig. 2*E*). Gavage of D-glucose increased V_{max} of GLUT2-mediated D-glucose uptake into BBMVs of wild-type mice 2.7-fold (168 ± 31 pmol × mg^{-1} × s^{-1}). Western blots using antibodies against GLUT2 from human (GLUT-Ab) that cross-react with mouse GLUT2 (21) showed a similar magnitude in the increase of GLUT2 protein expression in BBMVs of wild-type mice after the D-glucose bolus (Fig. 2*F*). The increase in both the GLUT2 protein expression and the GLUT2-mediated D-glucose uptake in response to the glucose bolus were blunted in *Sglt1*$^{-/-}$ mice. These findings are consistent with a role of SGLT1 in the upregulation of GLUT2 activity in the BBM by high glucose concentration.

Without D-glucose bolus the V_{max} of AMG uptake via SGLT1 was 5.5 times higher than maximal D-glucose uptake via GLUT2, and after glucose gavage the V_{max} of AMG
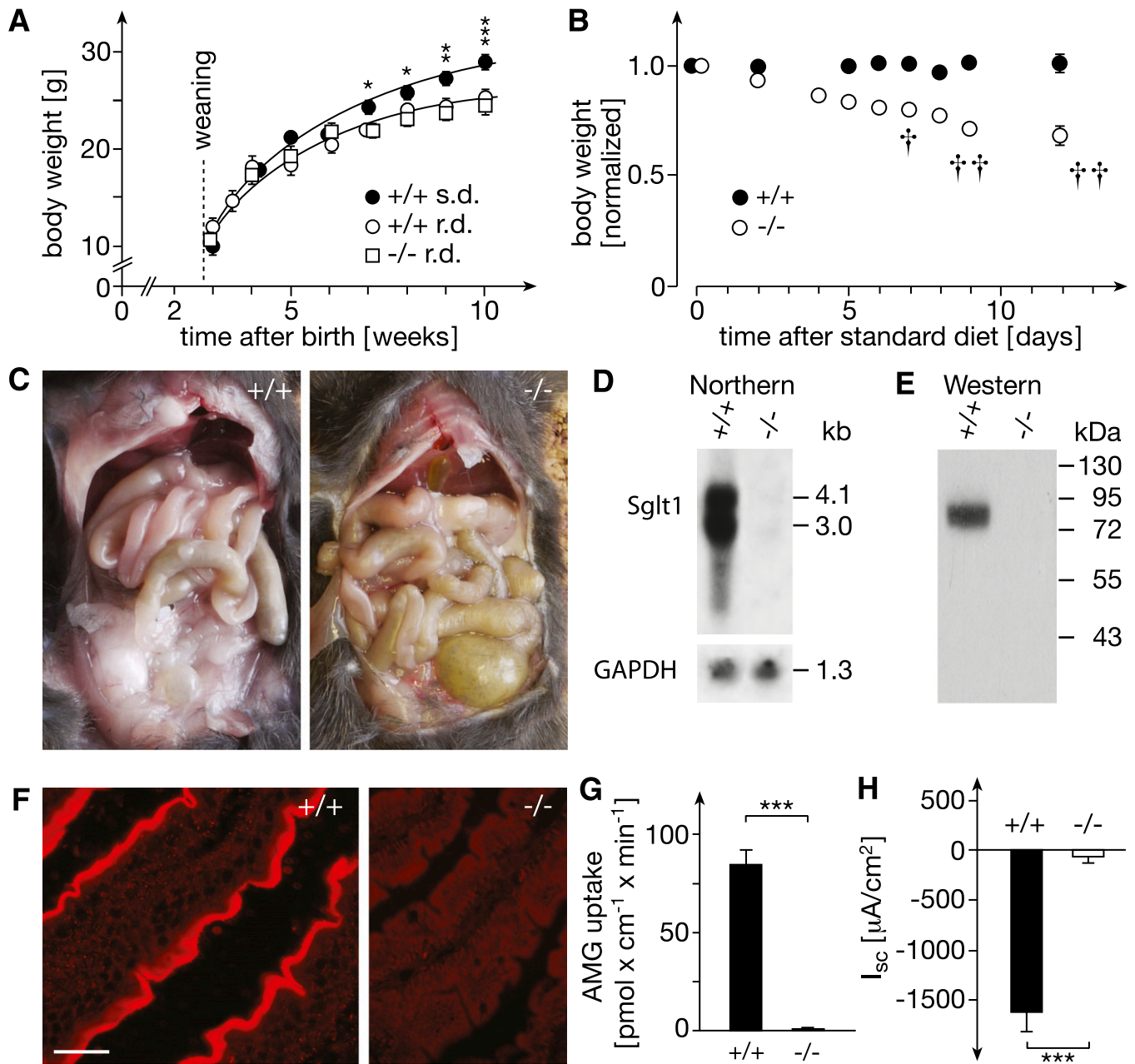
FIG. 1. Deletion of *Sglt1* in small intestine leads to GGM syndrome that can be prevented by a glucose-galactose–reduced diet. *A*: Body weight development after weaning. *Sglt1*^{+/−} mice receiving standard diet (s.d.) were bred. Newborn mice were genotyped 3 weeks after birth. After weaning, *Sglt1*^{+/+} and *Sglt1*^{−/−} mice were kept on standard diet or glucose/galactose-reduced diet (r.d.). Mean values ± SE of 8 animals are shown. *B*: Body weight development of 2-month-old mice that have been kept on glucose-galactose–reduced diet and were then switched to standard diet. Mean values ± SE are shown; *n* = 5 wild-type and 5 *Sglt1*^{−/−} mice (initial number of mice). †Death of one *Sglt1*^{−/−} mouse; ††Death of two *SGLT1*^{−/−} mice. *C*: Appearance of abdominal contents of 2-month-old mice kept on glucose-galactose–reduced diet after weaning that were fed 2 days with standard diet. *D*: Northern blots with mRNAs isolated from small intestines of 2-month-old mice hybridized with cDNA fragments of *Sglt1* or glyceraldehyde-3-phosphate dehydrogenase (GAPDH). A 176 bp *Sglt1* fragment comprising nucleotides 1727–1902 (accession number AF163846) and a 1.1 kb fragment of human GAPDH (Clontech, Heidelberg, Germany) was used. *E*: Western blots of small intestinal BBMs of 2-month-old mice, which were performed as described (28), were stained with antibody against SGLT1 (SGLT1-Ab, diluted 1:2,000). *F*: Immunohistochemistry of small intestine with SGLT1-Ab (dilution of SGLT1-Ab, 1:1,000; scale bar, 20 μm). G: Phlorizin-inhibitable uptake of 7 μmol/L AMG into enterocytes of everted rings of small intestine. Because phlorizin-inhibitable AMG uptake in duodenum and jejunum was not significantly different the measurements from both regions were combined. Mean values of phlorizin-inhibitable AMG uptake ± SE from four independent experiments are shown. *H*: D-glucose induced transepithelial short-circuit currents (I_{sc}). Small intestinal mucosa mounted into Ussing chambers was superfused at 37°C in the presence of 20 mmol/L mannitol or 20 mmol/L D-glucose, and electrogenic glucose uptake was measured as described (29). Mean values ± SE of five experiments. *$P < 0.05$, **$P < 0.01$, ***$P < 0.001$ determined by Student *t* tests. (A high-quality digital representation of this figure is available in the online issue.)

uptake via SGLT1 was 8.7 times higher compared with D-glucose uptake via GLUT2 (compare Fig. 2*C* and *E*). This indicates that D-glucose uptake via the luminal membrane of small intestinal enterocytes is predominantly (>80%) mediated via SGLT1.

SGLT1 is expressed in L-cells and K-cells. We investigated the expression of SGLT1 in enteroendocrine L-cells and K-cells, which are known to secrete GLP-1 and GIP, respectively (Fig. 4). Immunohistochemistry was performed using double staining with specific primary antibodies raised
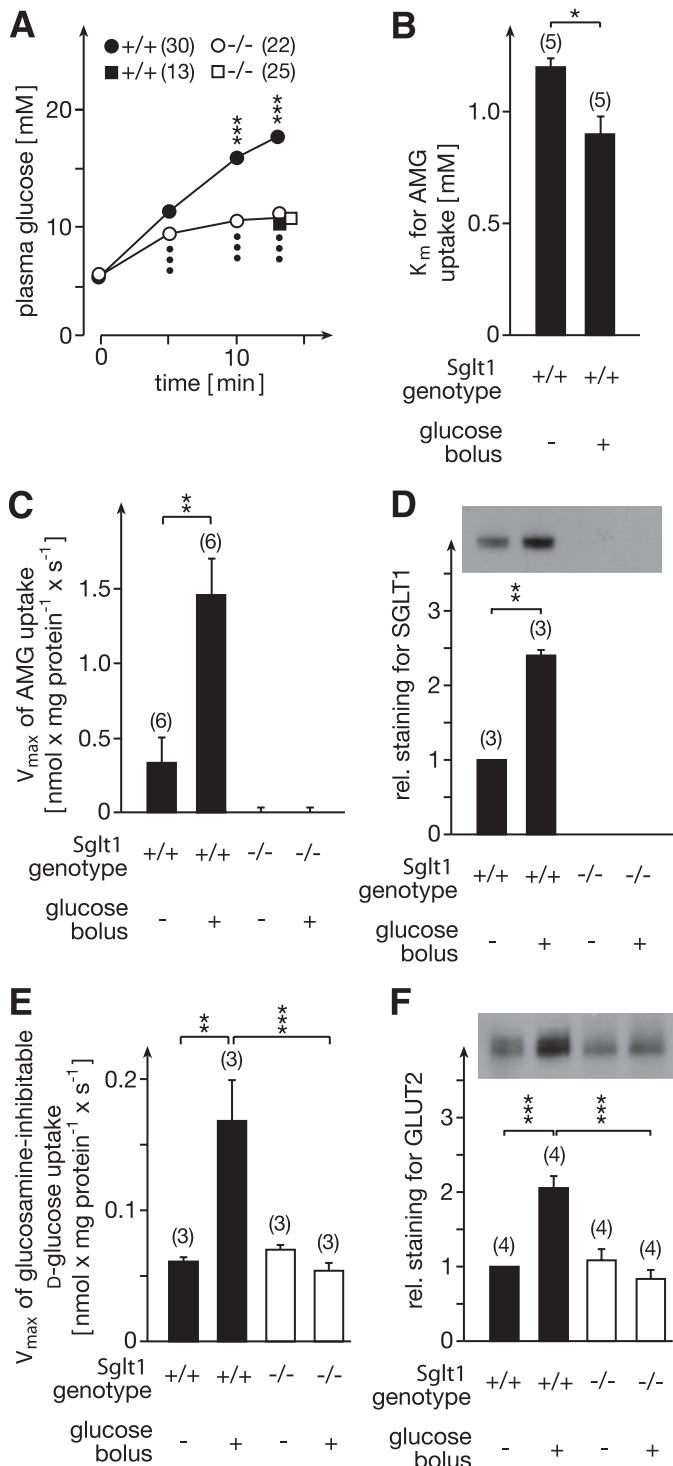
in rabbit or goat and fluorophore-labeled secondary antibodies raised in chicken. Fluorescence was visualized by laser scanning microscopy using an optical section thickness of 0.1 μm. Coexpression of SGLT1 with GLP-1 and GIP was observed in individual cells of jejunal crypts. SGLT1-Ab immunoreactivity was observed at the BBM of enteroendocrine cells, whereas immunoreactivities for antibodies against GIP or GLP-1 were predominantly observed in intracellular compartments (Fig. 4).

SGLT1 is required for elevated systemic blood concentrations of GIP and GLP-1 after gavage with D-glucose. Oral application of D-glucose stimulates the pancreatic secretion of insulin more than intravenous application. In humans, this surplus of insulin secretion is a result of the combined effects of GIP and GLP-1 (12,31). After exposure of the small intestine to high glucose the concentrations of these enterohormones increase in systemic blood.

Thirteen minutes after glucose gavage (2 mg/g body wt), plasma insulin was approximately two times higher in wild-type mice compared with $Sglt1^{-/-}$ mice (Fig. 5A). At the same time, GIP was increased ~10-fold in the systemic blood of wild-type mice but was not changed in $Sglt1^{-/-}$ mice (Fig. 5B). By comparison 13 min after gavage with olive oil (10 μL/g body wt), GIP increased four- to fivefold in the systemic blood of both wild-type and $Sglt1^{-/-}$ mice. Thirteen minutes after glucose gavage the active GLP-1 concentration in systemic blood was not increased in wild-type or $Sglt1^{-/-}$ mice, whereas application of oil induced a SGLT1-independent twofold increase in active GLP-1 (Fig. 5C). Because the concentration of active GLP-1 in systemic blood may be reduced by degradation we also measured total GLP-1 in the systemic blood 5 min after gavage of a greater D-glucose load (6 mg/g body wt; Fig. 5D). Under these conditions a significant glucose-dependent increase of GLP-1 concentration was observed in wild-type mice but not in $Sglt1^{-/-}$ mice. Measuring glucose-dependent stimulation of GIP and GLP-1 secretion from primary intestinal cultures prepared from $Sglt1^{+/-}$ and $Sglt^{-/-}$ mice, we confirmed that SGLT1 is required for glucose-dependent stimulation of these enterohormones (Supplementary Fig. 5).

SGLT1 in renal proximal tubules is required for complete reabsorption of filtered D-glucose. In kidney the low affinity Na^+-D-glucose cotransporter SGLT2 is located in BBMs of S1 segments of proximal tubules, whereas the high affinity Na^+-D-glucose cotransporter SGLT1 is located in BBMs of the S2 and S3 segments (20,22). We confirmed that no expression of SGLT1 was observed in kidneys of $Sglt1^{-/-}$ mice (Supplementary Figs.

FIG. 2. Upregulation of small intestinal D-glucose absorption after application of a D-glucose bolus to the stomach. *A*: D-glucose concentrations in the plasma after gavage with D-glucose (2 mg/g body wt; $Sglt1^{+/+}$, ●, $Sglt1^{-/-}$, ○) or buffer ($Sglt1^{+/+}$, ■; $Sglt1^{-/-}$, □). ****P* < 0.001, $Sglt1^{+/+}$ mice after glucose gavage vs. $Sglt1^{-/-}$ mice after glucose gavage; ●●●*P* < 0.001 differences to the D-glucose concentration in $Sglt1^{-/-}$ mice before glucose gavage. *B-F*: Properties of small intestine BBMVs of control $Sglt1^{+/+}$ and $Sglt1^{-/-}$ mice (−bolus) and of $Sglt1^{+/+}$ and $Sglt1^{-/-}$ mice that had received a D-glucose bolus (6 mg/g body wt) 30 min earlier (+bolus). *B*: K_m values for AMG of Na^+-dependent uptake of [^{14}C]AMG into BBMVs. Uptake rates were measured after incubation for 5 s in the presence of an inwardly directed gradient of 100 mmol/L NaSCN or 100 mmol/L KSCN, and the differences were calculated. *C*: Phlorizin-inhibitable uptake of AMG into BBMVs. Uptake of 0.1 mmol/L [^{14}C]AMG was measured after incubation for 2 s in the absence and presence of 200 μmol/L phlorizin, and the differences were calculated.

V_{max} values were calculated according to the Michaelis Menten equation using the K_m values determined in *B*. *D*: SGLT1 protein expressed in BBMVs. Western blots of BBMVs (26) were stained with SGLT1-Ab (diluted 1:2,000), and the staining was quantified by densitometry. *E*: Glucosamine-inhibitable uptake of D-glucose into BBMVs. Uptake rates of 100 mmol/L [^{3}H]D-glucose were measured in the absence and presence of 100 mmol/L D-glucosamine, and the differences were calculated. Because the Michaelis Menten constant (K_m) value of mouse GLUT2 for D-glucose is ~17 mmol/L (4), the uptake rates of 100 mmol/L D-glucose represent V_{max} values. *E*: GLUT2 protein expression in BBMVs. Western blots of BBMVs (27) were stained with antibody against human GLUT2 (diluted 1:500) cross-reacting with mouse GLUT2. Staining was quantified by densitometry. Means ± SE are presented. The number of independent experiments is indicated in parentheses. Significances of differences are calculated by ANOVA with post hoc Tukey comparison. **P* < 0.05; ***P* < 0.01; ****P* < 0.001; rel., relative.
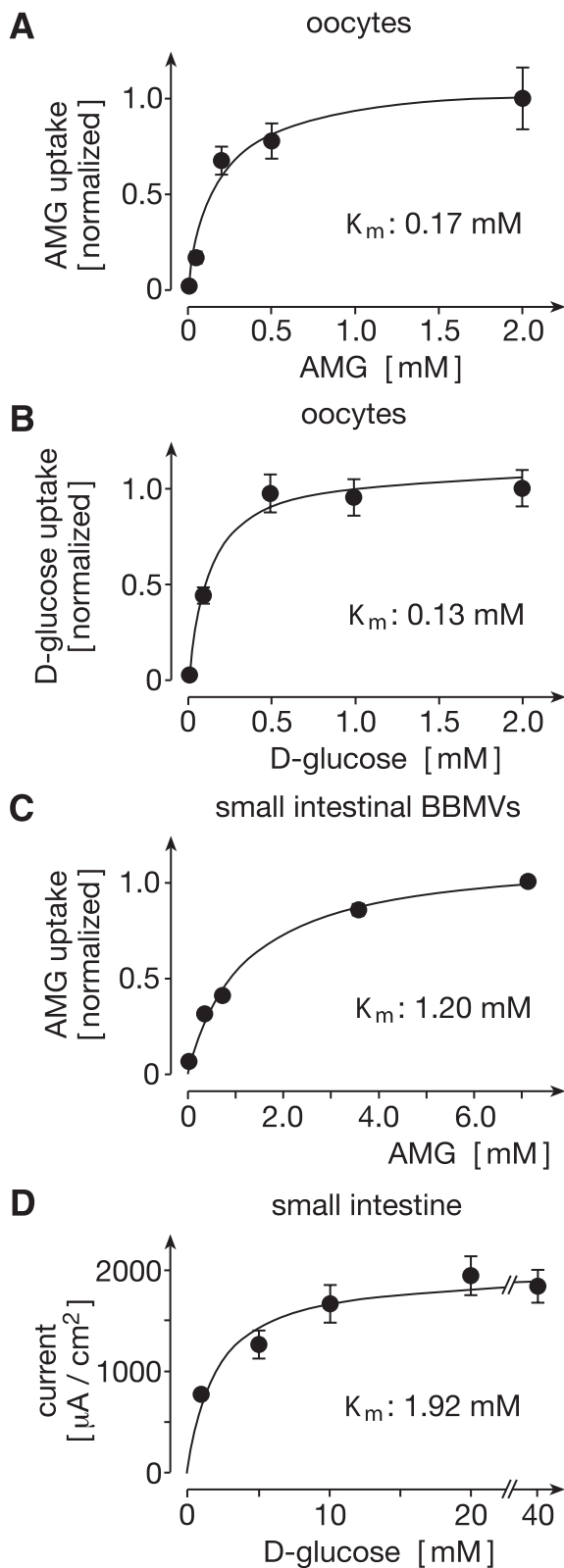
FIG. 3. **The substrate dependence of SGLT1-mediated glucose uptake expressed in oocytes is different from the substrate dependence of SGLT1-mediated glucose uptake across small intestinal BBM.** *A* **and** *B:* **Transport measurements in oocytes. Oocytes were injected with 5 ng of mouse** *Sglt1* **cRNA and incubated 2 days for expression. Uptake of different concentrations of [14C]AMG (*A*) or [3H]D-glucose (*B*) was measured in the absence and presence of 100 µmol/L phlorizin. Phlorizin-inhibitable uptake rates of individual experiments were normalized to the uptake rates measured at 2 mmol/L AMG or D-glucose. Mean values ± SE of 25–30 oocytes from 3 independent experiments are shown. Similar**

6*A* and 7*A*) and determined at mRNA and protein levels that the expression of SGLT2 was not changed after removal of SGLT1 (Supplementary Figs. 6*B* and 7*B* and *C*). In wild-type and *Sglt1*$^{-/-}$ mice similar mRNA and protein concentrations of the passive glucose transporters GLUT1, GLUT2, and GLUT5 were determined (Supplementary Fig. 7*B* and *C*).

Spontaneous urine collections in awake male mice revealed that urinary glucose concentrations were significantly increased in *Sglt1*$^{-/-}$ compared with wild-type mice, whereas blood glucose levels were not different (Fig. 6*A*). Fractional glucose reabsorption was 100% in male wild-type and 97% in male *Sglt1*$^{-/-}$ mice (Fig. 6*B*). In male mice, GFR measured in awake and anesthetized animals, blood pressure, heart rate, plasma urea concentrations, food intake and fluid intake, and renal excretion of fluid, Na$^+$, and Cl$^-$ were not changed after removal of SGLT1. Details and differences in food intake and fluid intake between males and females are described in the Supplementary Data.

Quantitative free-flow collections of tubular fluid were performed from the last surface loop of proximal convoluted tubules. Mean values for single nephron GFR and the amount of glucose filtered per nephron were not different between male *Sglt1*$^{-/-}$ and wild-type mice (Fig. 7*A* and *B*). However, the concentration and delivery of glucose were increased in *Sglt1*$^{-/-}$ versus wild-type mice, whereas fractional glucose reabsorption was reduced (Fig. 7*C* and *D*). In contrast with fractional reabsorption of glucose, fractional reabsorption of fluid and chloride was not significantly different between male *Sglt1*$^{-/-}$ and wild-type mice (fluid: 0.48 ± 0.02 vs. 0.45 ± 0.03; chloride: 0.47 ± 0.03 vs. 0.45 ± 0.03; *n* = 17–25 nephrons in each group, not significant).

DISCUSSION

In the current study the role of SGLT1 for small intestinal glucose absorption and incretin secretion was investigated comparing nondiabetic mice without and with expression of SGLT1. Evidence is presented that SGLT1 mediates the majority of D-glucose transport across the BBM of enterocytes independent of the glucose load. SGLT3b, a second functional Na$^+$-D-glucose cotransporter in the BBM of

apparent K_m values of 0.17 ± 0.05 mmol/L and 0.13 ± 0.01 mmol/L were obtained for AMG and D-glucose, respectively. The V_{max} values of SGLT1-mediated uptake of AMG and D-glucose were similar. In oocytes of the same batch, which were injected with 5 ng of *Sglt1* cRNA per oocyte and incubated for 2 days, V_{max} values (measured at monosaccharide concentrations of 2 mmol/L without and with 100 µmol/L phlorizin) of 5.0 ± 0.6 (AMG) and 4.8 ± 0.6 (D-glucose) pmol × oocyte^{-1} × min^{-1} were obtained (*n* = 25 each, not significant). *C:* Transport measurements in BBMVs. Wild-type mice fed with standard diet were starved for 18 h and killed at 3–4 P.M. BBMVs were prepared. BBMVs were incubated for 2 s at 37°C with different concentrations of [14C]AMG in the presence of an inwardly directed gradient of 100 mmol/L NaSCN or 100 mmol/L KSCN. The sodium-dependent uptake rates of individual experiments were normalized to the values obtained at 10 mmol/L AMG. Mean values ± SE of 12 measurements from three independent experiments are shown. A K_m value of 1.20 ± 0.04 mmol/L (*n* = 5) was determined. *D:* Glucose-induced short circuit currents across small intestinal mucosa. Wild-type mice fed with standard diet were starved for 18 h and killed at 4 P.M. The jejunal small intestinal wall was then mounted to an Ussing chamber. The mucosal side was superfused with different concentrations of D-glucose, and D-glucose–induced short circuit currents (I_{sc}) mediated by Na$^+$-D-glucose cotransport was measured. Mean values ± SE of 7 experiments are shown. The Michaelis Menten equation was fitted to the data. A K_m value of 1.9 ± 0.6 mmol/L was determined.
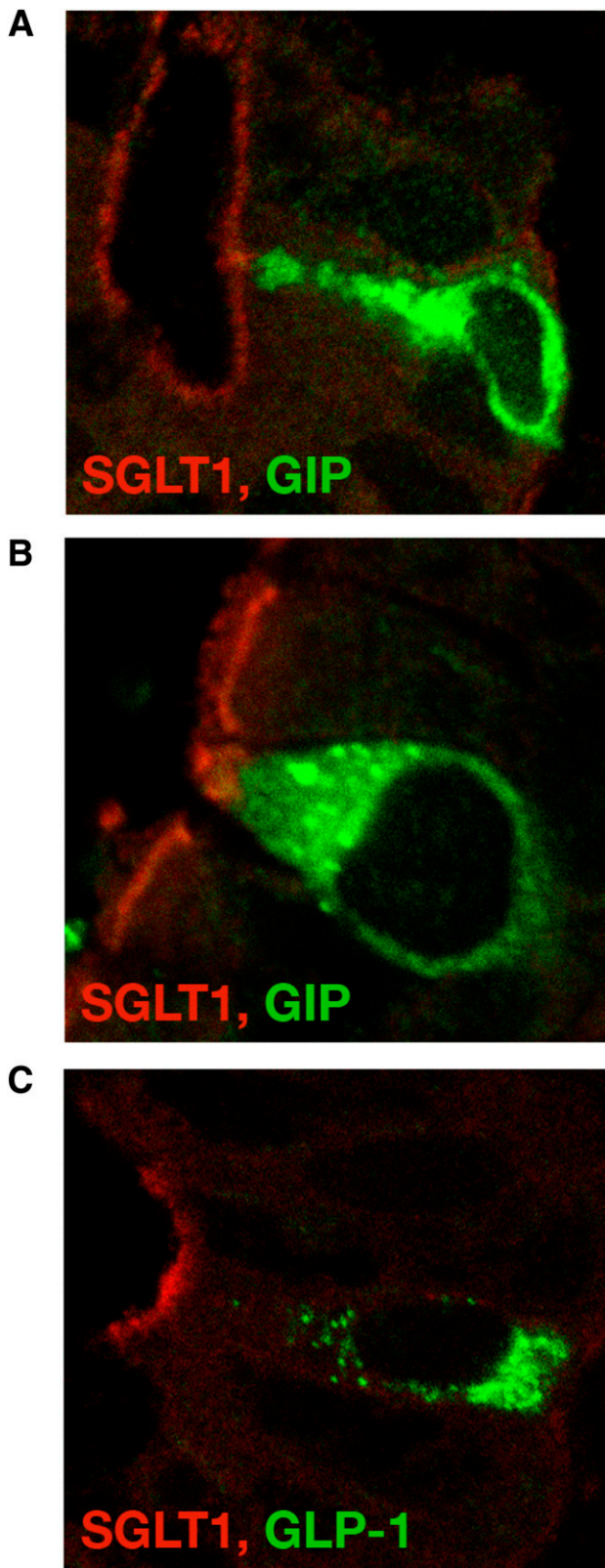
FIG. 4. Expression of SGLT1 in enteroendocrine cells. Sections from jejunum of mice were first incubated with antibodies against GIP or GLP-1 raised in goat and then with SGLT1-Ab raised in rabbit (GIP-Ab and GLP-1 were diluted 1:100, and SGLT1-Ab diluted 1:1,000). Staining was performed with fluorescent-labeled secondary antibodies (diluted 1:800) against goat IgG (GIP or GLP-1, green) and rabbit IgG (SGLT1, red). *A* and *B*: K-cell in crypts. *C*: L-cell in a crypt. Scale bar, 5 μm. (A high-quality digital representation of this figure is available in the online issue.)
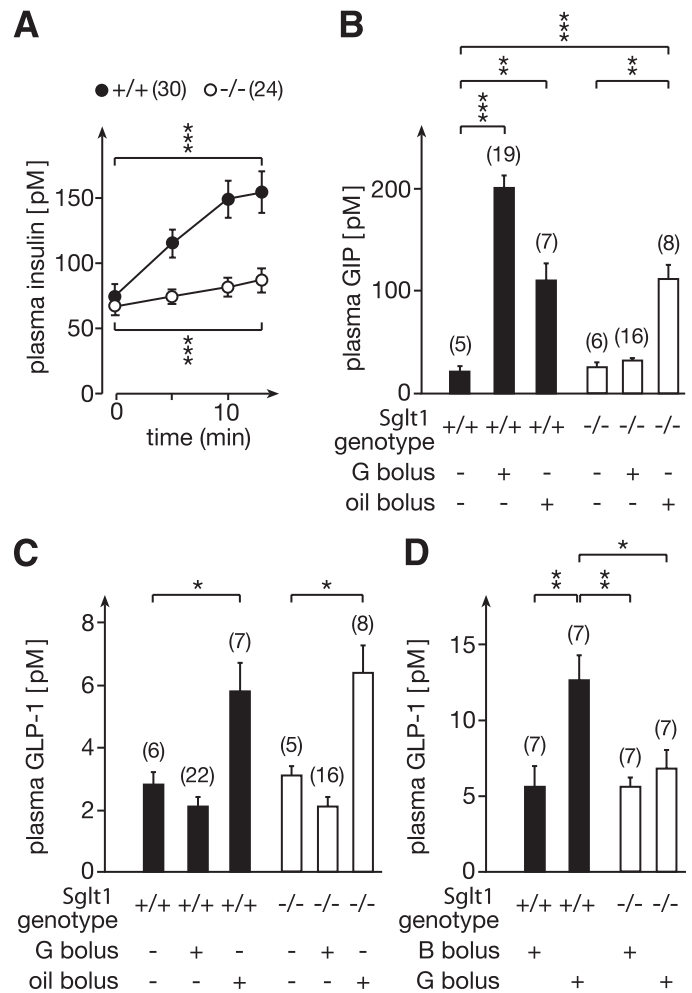
FIG. 5. Secretion of insulin, GIP, and GLP-1 after gavage with D-glucose in $Sglt1^{-/-}$ mice versus $Sglt^{+/+}$ mice. *A*: Effect of D-glucose gavage (2 mg/g body wt) on systemic plasma insulin concentrations. *B*: Concentrations of GIP in systemic blood plasma before and 13 min after gavage with D-glucose (G bolus; 2 mg/g body wt) or 13 min after gavage with oil (10 μL/g body wt). *C*: Concentrations of active GLP-1 in systemic blood plasma before and 13 min after gavage with D-glucose (2 mg/g body wt) or oil. *D*: Concentration of total GLP-1 in systemic blood plasma 5 min after gavage with PBS (B bolus) or D-glucose (G bolus; 6 mg/g body wt). $*P < 0.05$, $**P < 0.01$, $***P < 0.001$, Student t tests.

mice, does not contribute significantly. After high glucose load some GLUT2 is incorporated into the BBM, but this has minor impact on small intestinal glucose absorption. It is noteworthy that this translocation of GLUT2 was not observed in $Sglt1^{-/-}$ mice, indicating that SGLT1 rather than sweet taste receptors is pivotal in this upregulation (5,6,8). Without and with D-glucose load the capacity of SGLT1 versus GLUT2 for D-glucose transport across the BBMs was 5.5 and 8.7 times higher, respectively. In response to continuous feeding of sugar-rich diets and during diabetes, however, the contribution of GLUT2 to small intestinal glucose absorption may become more relevant. Under these conditions the expression of SGLT1 and GLUT2 is increased, and an increase of GLUT2 in the BBM was observed after gavage with glucose or fructose (32–35).

Removal of SGLT1 in mice resulted in GGM syndrome (OMIM 182380) that could be cured by a glucose-galactose–reduced diet as has been observed in patients
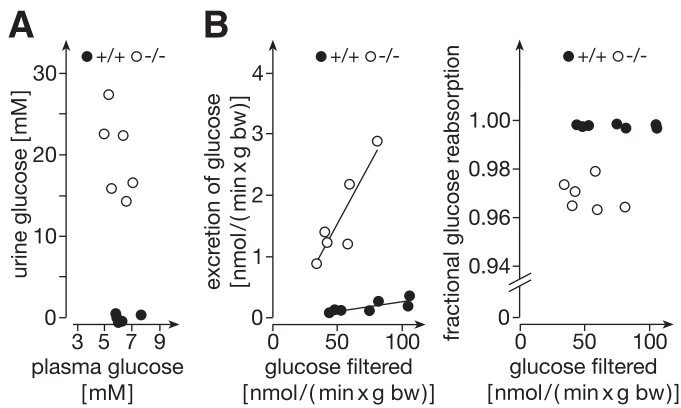
FIG. 6. Effects of SGLT1 removal on renal glucose excretion. *A*: D-glucose concentrations measured in spontaneous urine collections and subsequently obtained blood collections from tail vein of awake male mice (for experimental details [29]). *B*: Absolute renal excretion and fractional reabsorption of glucose in male *Sglt1⁻/⁻* versus *Sglt1⁺/⁺* mice as function of the amount of filtered glucose. GFR was measured in awake mice using the plasma kinetics of FITC-inulin after a single dose intravenous injection (26). Mean values ± SE are shown. bw, Body weight.

cells staining positive for the incretin hormones, GLP-1 and GIP. Active forms of GLP-1 and GIP are detectable in the systemic blood of human subjects after glucose ingestion (38,39), but are rapidly inactivated in the circulation by DPP-IV (10). Both GIP and GLP-1 trigger glucose-dependent insulin secretion, and although the effectiveness of GIP is impaired in people with type 2 diabetes (40), the preserved insulinotropic effect of GLP-1 (40) has led to the successful development of GLP-1 mimetics and DPP-IV inhibitors as new classes of antidiabetic agent (41). Earlier in vitro studies have demonstrated that SGLT1-mediated monosaccharide transport triggers incretin secretion via the electrogenic coupled influx of Na^+, which results in membrane depolarization, electrical activity, voltage-gated Ca^{2+} entry, and exocytosis (16,42), although the contribution of this pathway to glucose-mediated secretion in vivo has remained controversial. Using the SGLT1⁻/⁻ mice we now demonstrate the pivotal role of SGLT1 for both GLP-1 and GIP secretory responses triggered by oral glucose in vivo. This is consistent with the reported phlorizin sensitivity of glucose-induced incretin increases in the portal vein (13) showing the involvement of a phlorizin-sensitive SGLT-type transporter or channel (3,30,43), as well as with the finding that incretin secretion is triggered in vivo by substrates of SGLT1 (44), but not by other sweet tasting compounds (14). The results suggest that secretion of these hormones would be initiated after food ingestion by the early arrival of even small glucose loads in the small intestine, consistent with previous reports that GLP-1 release is initiated in humans when glucose infusion rates exceed the absorption capacity of the duodenum (45).

Whereas glucose is nearly completely reabsorbed by the kidneys in wild-type mice, *Sglt1⁻/⁻* mice lose ~3% of the filtered glucose in the urine, leading to a urinary D-glucose concentration of ~20 mmol/L. Notably *Sglt2* null mice lose only ~60% of the filtered glucose in the urine although the expression of SGLT1 was downregulated by 50% (20). This suggests that wild-type mice do not use the maximal transport capacity of SGLT1 at normoglycemic conditions. This is different when the glucose load to the SGLT1-expressing
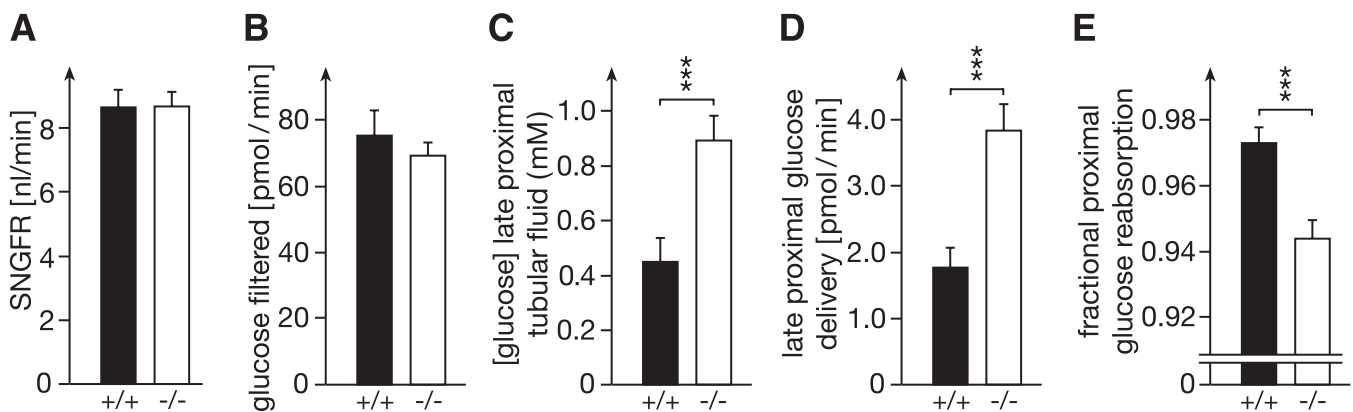
with loss-of-function mutations in SGLT1 (*SLC5A1*) (18,19). GGM is characterized by severe diarrhea and dehydration as a result of osmotic loss by retention of nonabsorbed D-glucose, D-galactose, and sodium in the small intestinal lumen. In contrast with humans, where severe diarrhea and dehydration are observed in suckling neonates, suckling *Sglt1⁻/⁻* mice showed no obvious symptoms. This species difference may be explained by the three to four times higher concentrations of lactose in human milk compared with murine milk (36,37). In the small intestine lactose is degraded by lactase-isomaltase and provides the only relevant source of D-glucose and D-galactose in suckling neonates.

Confirming previous results (15,16) we showed that SGLT1 is expressed in the luminal membrane of enteroendocrine

FIG. 7. Micropuncture studies in male wild-type and *Sglt1⁻/⁻* mice. Mice were anesthetized with thiobutabarbital (100 mg/kg i.p.) plus ketamine (100 mg/kg i.m.) and prepared for renal micropuncture as described (20,27). A catheter was placed in the femoral artery for continuous blood pressure recording, and a bladder catheter was applied for urine collections. For assessment of GFR, [³H]inulin was added to the infusion to deliver 20 μCi/h and urine was quantitatively collected. To determine proximal glucose reabsorption, quantitative free-flow fluid collections were made from the last surface loop of proximal convoluted tubules and tubular fluid volume was determined from transfer to a constant bore capillary. Concentrations of glucose in plasma, urine, and tubular fluid were determined as described (27). *A*: GFRs of single nephrons (SNGFR). *B*: Filtration of D-glucose by single nephrons. *C*: D-glucose concentrations in the last surface loops of proximal tubules. *D*: Amount of D-glucose delivered to the last surface loops of proximal tubules. *E*: Fractional reabsorption of D-glucose up to the last proximal tubular surface loops. Nephrons (2–25) in five to six mice/genotype were investigated. Mean values ± SE are shown. ***$P < 0.001$, Student *t* tests.

S2 and S3 segments is increased. In diabetic patients in which early proximal tubule glucose transport capacity is overwhelmed by high D-glucose concentrations, and even more in diabetic patients treated with an SGLT2 specific inhibitor, SGLT1 may operate at full transport capacity (17).

The *Sglt1* null mice provide a valuable tool for future studies of SGLT1 functions under pathological conditions as well as the therapeutic potential of SGLT1 inhibition.

REFERENCES

1. Marsenic O. Glucose control by the kidney: an emerging target in diabetes. Am J Kidney Dis 2009;53:875–883
2. Brubaker PL. Incretin-based therapies: mimetics versus protease inhibitors. Trends Endocrinol Metab 2007;18:240–245
3. Wright EM, Loo DDF, Hirayama BA. Biology of human sodium glucose transporters. Physiol Rev 2011;91:733–794
4. Uldry M, Thorens B. The SLC2 family of facilitated hexose and polyol transporters. Pflugers Arch 2004;447:480–489
5. Kellett GL. The facilitated component of intestinal glucose absorption. J Physiol 2001;531:585–595
6. Kellett GL, Brot-Laroche E, Mace OJ, Leturque A. Sugar absorption in the intestine: the role of GLUT2. Annu Rev Nutr 2008;28:35–54
7. Margolskee RF, Dyer J, Kokrashvili Z, et al. T1R3 and gustducin in gut sense sugars to regulate expression of Na$^+$-glucose cotransporter 1. Proc Natl Acad Sci USA 2007;104:15075–15080
8. Kellett GL, Brot-Laroche E. Apical GLUT2: a major pathway of intestinal sugar absorption. Diabetes 2005;54:3056–3062
9. Stümpel F, Burcelin R, Jungermann K, Thorens B. Normal kinetics of intestinal glucose absorption in the absence of GLUT2: evidence for a transport pathway requiring glucose phosphorylation and transfer into the endoplasmic reticulum. Proc Natl Acad Sci USA 2001;98:11330–11335
10. Holst JJ. The physiology of glucagon-like peptide 1. Physiol Rev 2007;87:1409–1439
11. Brubaker PL. The glucagon-like peptides: pleiotropic regulators of nutrient homeostasis. Ann N Y Acad Sci 2006;1070:10–26
12. Baggio LL, Drucker DJ. Biology of incretins: GLP-1 and GIP. Gastroenterology 2007;132:2131–2157
13. Moriya R, Shirakura T, Ito J, Mashiko S, Seo T. Activation of sodium-glucose cotransporter 1 ameliorates hyperglycemia by mediating incretin secretion in mice. Am J Physiol Endocrinol Metab 2009;297:E1358–E1365
14. Fujita Y, Wideman RD, Speck M, et al. Incretin release from gut is acutely enhanced by sugar but not by sweeteners in vivo. Am J Physiol Endocrinol Metab 2009;296:E473–E479
15. Parker HE, Habib AM, Rogers GJ, Gribble FM, Reimann F. Nutrient-dependent secretion of glucose-dependent insulinotropic polypeptide from primary murine K cells. Diabetologia 2009;52:289–298
16. Reimann F, Habib AM, Tolhurst G, Parker HE, Rogers GJ, Gribble FM. Glucose sensing in L cells: a primary cell study. Cell Metab 2008;8:532–539
17. Vallon V, Sharma K. Sodium-glucose transport: role in diabetes mellitus and potential clinical implications. Curr Opin Nephrol Hypertens 2010;19:425–431
18. Lindquist B, Meeuwisse G, Melin K. Glucose-galactose malabsorption. Lancet 1962;2:666
19. Wright EM, Turk E, Martin MG. Molecular basis for glucose-galactose malabsorption. Cell Biochem Biophys 2002;36:115–121
20. Vallon V, Platt KA, Cunard R, et al. SGLT2 mediates glucose reabsorption in the early proximal tubule. J Am Soc Nephrol 2011;22:104–112
21. Miettinen PJ, Ustinov J, Ormio P, et al. Downregulation of EGF receptor signaling in pancreatic islets causes diabetes due to impaired postnatal β-cell growth. Diabetes 2006;55:3299–3308
22. Balen D, Ljubojevic M, Breljak D, et al. Revised immunolocalization of the Na$^+$-D-glucose cotransporter SGLT1 in rat organs with an improved antibody. Am J Physiol Cell Physiol 2008;295:C475–C489
23. Hopfer U, Nelson K, Perrotto J, Isselbacher KJ. Glucose transport in isolated brush border membrane from rat small intestine. J Biol Chem 1973;248:25–32
24. Uldry M, Ibberson M, Hosokawa M, Thorens B. GLUT2 is a high affinity glucosamine transporter. FEBS Lett 2002;524:199–203
25. Veyhl M, Keller T, Gorboulev V, Vernaleken A, Koepsell H. RS1 *(RSC1A1)* regulates the exocytotic pathway of Na$^+$-D-glucose cotransporter SGLT1. Am J Physiol Renal Physiol 2006;291:F1213–F1223
26. Vallon V, Schroth J, Satriano J, Blantz RC, Thomson SC, Rieg T. Adenosine A$_1$ receptors determine glomerular hyperfiltration and the salt paradox in early streptozotocin diabetes mellitus. Nephron Physiol 2009;111:30–38
27. Vallon V, Grahammer F, Volkl H, et al. KCNQ1-dependent transport in renal and gastrointestinal epithelia. Proc Natl Acad Sci USA 2005;102:17864–17869
28. Keller T, Elfeber M, Gorboulev V, Reiländer H, Koepsell H. Purification and functional reconstitution of the rat organic cation transporter OCT1. Biochemistry 2005;44:12253–12263
29. Grahammer F, Henke G, Sandu C, et al. Intestinal function of gene-targeted mice lacking serum- and glucocorticoid-inducible kinase 1. Am J Physiol Gastrointest Liver Physiol 2006;290:G1114–G1123
30. Aljure O, Díez-Sampedro A. Functional characterization of mouse sodium/glucose transporter type 3b. Am J Physiol Cell Physiol 2010;299:C58–C65
31. Nauck MA, Bartels E, Ørskov C, Ebert R, Creutzfeldt W. Additive insulinotropic effects of exogenous synthetic human gastric inhibitory polypeptide and glucagon-like peptide-1-(7-36) amide infused at near-physiological insulinotropic hormone and glucose concentrations. J Clin Endocrinol Metab 1993;76:912–917
32. Shirazi-Beechey SP, Hirayama BA, Wang Y, Scott D, Smith MW, Wright EM. Ontogenic development of lamb intestinal sodium-glucose co-transporter is regulated by diet. J Physiol 1991;437:699–708
33. Gouyon F, Caillaud L, Carrière V, et al. Simple-sugar meals target GLUT2 at enterocyte apical membranes to improve sugar absorption: a study in GLUT2-null mice. J Physiol 2003;552:823–832
34. Tobin V, Le Gall M, Fioramonti X, et al. Insulin internalizes GLUT2 in the enterocytes of healthy but not insulin-resistant mice. Diabetes 2008;57:555–562
35. Miyamoto K-I, Hase K, Takagi T, et al. Differential responses of intestinal glucose transporter mRNA transcripts to levels of dietary sugars. Biochem J 1993;295:211–215
36. Miller JB, Bull S, Miller J, McVeagh P. The oligosaccharide composition of human milk: temporal and individual variations in monosaccharide components. J Pediatr Gastroenterol Nutr 1994;19:371–376
37. Ragueneau S. Early development in mice. IV: Quantity and gross composition of milk in five inbred strains. Physiol Behav 1987;40:431–435
38. Herrmann C, Göke R, Richter G, Fehmann HC, Arnold R, Göke B. Glucagon-like peptide-1 and glucose-dependent insulin-releasing

polypeptide plasma levels in response to nutrients. Digestion 1995; 56:117–126

39. Theodorakis MJ, Carlson O, Michopoulos S, et al. Human duodenal enteroendocrine cells: source of both incretin peptides, GLP-1 and GIP. Am J Physiol Endocrinol Metab 2006;290:E550–E559

40. Nauck MA, Heimesaat MM, Orskov C, Holst JJ, Ebert R, Creutzfeldt W. Preserved incretin activity of glucagon-like peptide 1 [7-36 amide] but not of synthetic human gastric inhibitory polypeptide in patients with type-2 diabetes mellitus. J Clin Invest 1993;91:301–307

41. Drucker DJ, Nauck MA. The incretin system: glucagon-like peptide-1 receptor agonists and dipeptidyl peptidase-4 inhibitors in type 2 diabetes. Lancet 2006;368:1696–1705

42. Gribble FM, Williams L, Simpson AK, Reimann F. A novel glucose-sensing mechanism contributing to glucagon-like peptide-1 secretion from the GLUTag cell line. Diabetes 2003;52:1147–1154

43. Diez-Sampedro A, Hirayama BA, Osswald C, et al. A glucose sensor hiding in a family of transporters. Proc Natl Acad Sci USA 2003;100: 11753–11759

44. Ritzel U, Fromme A, Ottleben M, Leonhardt U, Ramadori G. Release of glucagon-like peptide-1 (GLP-1) by carbohydrates in the perfused rat ileum. Acta Diabetol 1997;34:18–21

45. Schirra J, Katschinski M, Weidmann C, et al. Gastric emptying and release of incretin hormones after glucose ingestion in humans. J Clin Invest 1996; 97:92–103